This manuscript is a non-peer reviewed preprint and has been submitted to EarthArXiv. It is under peer review at *Nature Communications*. Please feel free to contact any of the authors directly to comment on the manuscript.

27th October 2022

Quantitative constraints on flood variability in the rock record.

Jonah S. McLeod[1]*, James Wood[1], Sinead J. Lyster[1,2], Jeffrey M. Valenza[3], Alan R.T. Spencer[1,4], Alexander C. Whittaker[1].

[1]Department of Earth Science and Engineering, Imperial College London, UK, SW7 2BX.

[2] Department of Geosciences, The Pennsylvania State University, State College, Pennsylvania 16801, USA.

[3]Department of Geography, University of California, Santa Barbara, 1832 Ellison Hall, Santa Barbara, California 93106, USA.

[4]Science Group, The Natural History Museum, London, UK, SW7 5HD.

*jonah.mcleod18@imperial.ac.uk

ORCiDs: JSM – 0000-0002-5382-3559, JW – 0000-0002-1673-0097, SJL - 0000-0002-1188-533X, JMV - 0000-0002-1066-0817, ARTS - 0000-0001-6590-405X, ACW - 0000-0002-8781-7771

Abstract

Floods determine river behaviour in time and space. Yet quantitative measures of discharge variability from geological stratigraphy are sparse, even though they are critical to understand landscape sensitivity to past and future environmental change. Here we show how climate-driven floods in rivers in the geologic past can be quantified, using Carboniferous stratigraphy as an exemplar. Mass-preservation of woody debris coupled with the geometries of dune cross-sets demonstrate discharge-driven disequilibrium dynamics dominated fluvial deposition. Based on preserved bedforms, we quantified the magnitude and duration of flow variability, showing that rivers were perennial but prone to flashy floods lasting 4-16 hours. This is the largest stratigraphic interval over which disequilibrium bedform preservation has been documented and it demonstrates how climate-driven sedimentation events can be quantified in the geological past. We argue that signals of flooding may be ubiquitous but under-recognised in the rock record, indicating a significant preservation bias.

1 Introduction

Rivers are the most significant drivers of water and sediment transport across the continents[1,2], and associated flood events play a key role in shaping landscapes, impacting ecosystems, and determining the magnitude, characteristics and locus of sedimentation on the surface of the Earth[3–13]. In principle, fluvial strata, which constitute a physical record of ancient river behaviour, provide a key archive to assess the impacts of flooding in the geologic past. An outstanding research challenge for geoscientists is to decode this archive effectively to evaluate: how, where and when fluvial deposits may record extreme events; the extent to which they can be quantified; and the extent to which they may dominate the stratigraphic record[10,14–16]. This is particularly important as constraints on discharge variability from the geologic record provide a critical tool to understand past impacts of climate variability on river behaviour, e.g.[11,17,18]. To-date qualitative insights into flow variability have largely been extracted from the rock record using facies analysis[13,19–23]. However, recent advances in our understanding of fluvial bedform dynamics in disequilibrium conditions raise the possibility of gaining quantitative insights into flow variability in ancient rivers; when used together with sedimentary observations, these advances permit reconstruction of flood magnitudes and variability directly from fluvial stratigraphy.

The approach begins with the fundamental morphometrics of fluvial bedforms[9,24–31], in particular dune-scale cross-strata, which are ubiquitous in many ancient river deposits[9,24,27–29]. Cross-sets are preserved when dunes are not fully reworked by the prevailing flow, allowing the remaining bedform to become buried (Fig. 1). The "flood hypothesis" of bedform preservation[16] states that enhanced bedform preservation occurs during floods (especially those with flashy hydrographs) when the formative flood duration, T_f, is less than the timescale to rework a bedform, known as the turnover timescale, T_t (Fig. 1, see Table 1 for definitions). This is due to hysteresis in the adjustment of bedforms to changing flow conditions, meaning that when $T_f < T_t$, bedforms do not have time to adjust in form to reach equilibrium with the prevailing flow. This key signal of flow variability can be extracted from dune-scale cross-strata by using measurements of the distribution of heights (h_{xs}) of preserved cross-sets to calculate their coefficient of variation *CV*[16]. In steady-state flow conditions, which may occur when $T_f \geq T_t$, the spread in cross-set heights in preserved stratigraphy is high: the *CV* is expected to be in the range 0.88 ± 0.3 because theory and experiments demonstrate that bedform migration across random bed topography with low angles of climb, in equilibrium with the prevailing flow, results in low bedform preservation and high *CV* (Fig. 1a) [16,24–26]. In contrast, when preservation occurs in disequilibrium conditions, which may arise due to flooding, the opposite is true (Fig. 1b). Here, limited reworking of sediment within a dune results in lower *CV* [29], with a greater proportion of the original dune is preserved in stratigraphy. To-date the flood hypothesis for enhanced preservation has not been explicitly verified in the geologic record[9,31]. This is because flow variability is not the only origin of disequilibrium conditions: enhanced bedform preservation in disequilibrium conditions can also be caused by the presence of morphodynamic hierarchy, such as dunes migrating atop barforms[29,34]. Here, however, we test the flood hypothesis for enhanced bedform preservation in a location where unambiguous evidence of variable discharge conditions, including mass preservation of woody debris, can be combined with our quantitative bedform and palaeohydrologic analyses. Consequently, we demonstrate how sophisticated insights into water fluxes, climate and discharge variability can now be quantified for the geological past from stratigraphic data.

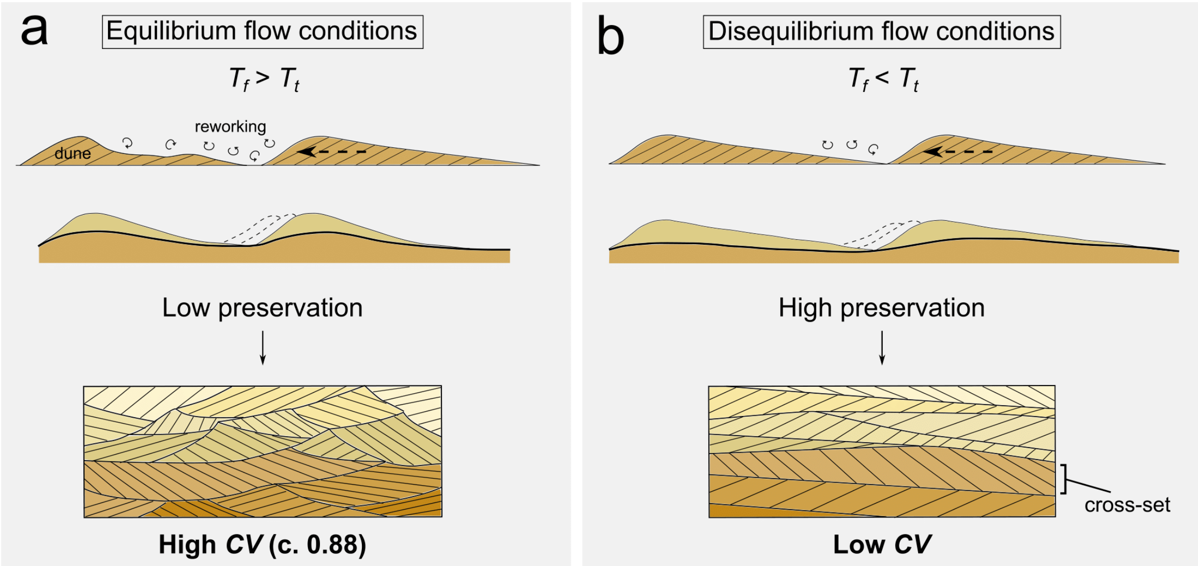

Figure 1: The hydrodynamic conditions that lead to differences in coefficient of variation of cross-set height, *CV*, recorded in cross-strata. (a) Dune migration and evolution in steady-state (equilibrium) flow conditions, and the resultant geometries of preserved cross-sets; (b) dune evolution and preservation in disequilibrium with prevailing flow, resulting in low *CV*.

Parameter	Definition		References
Mean cross set height, h_{xs}	The mean height of a set of heights measured along the dip-section of a cross-set.		24,25
Original bedform height, h_d	The original height of the bedform before preservation as a cross-set.		
	$h_d = 2.9(\pm 0.7)h_{xs}$		
Bedform preservation ratio, h_{xs}/h_d	The ratio of cross-set height to original bedform height, representing the proportion of the original height of the bedform preserved in the rock record.		9,16
Coefficient of variation of cross-set height, CV	The ratio of standard deviation to mean of cross-set height, measured along a single cross-set.		24,25
	$CV = \frac{s}{m}$	σ: standard deviation μ: mean	
Bedform turnover timescale, T_t	The length of time taken for a bedform to be fully reworked by flow, or for the sediment in a dune to be displaced downstream by one bedform wavelength.		15,16,32
	$T_t = \frac{\lambda h_d \beta}{q_b}$	λ: dune wavelength (≈7.3H) β: shape factor (≈0.55) q_b: unit bedload flux	
Prevailing flow duration, T_f	The duration of the falling limb of the discharge event which generated the preserved bedform.		15,16
	$T_f = T_t T*$	$T*$: bedform disequilibrium number	
Flow intermittency factor, I_f	The fraction of the total time in which bankfull flow would accomplish the same amount of water discharge as the real hydrograph.		33

	$I_f = \frac{\Sigma Q(t)}{Q_{bf}\Sigma t}$	$\Sigma Q(t)$: sum of the time dependent discharge Q_{bf}: bankfull discharge Σt: timespan	

Table 1: Key palaeohydrological variables and their definitions.

2. Study Area

We focus on the Pennant Formation of South Wales, UK (Figs 2, 3), a 1.3 km thick succession of Upper Carboniferous (Bolsovian–Asturian stages; 312.4–308 Ma) fluvial strata[36,37]. The five members of the formation (Llynfi, Rhondda, Brithdir, Hughes, Swansea – see Fig. 2) were deposited when South Wales was located near the equator, at a palaeolatitude of between 2.7°N and 3.0°S[38]. The formation is the product of rivers that drained the Variscan Mountains, flowing north-west[31] across foreland basin floodplains[34,39]. The regional climate was warm and wet, with precipitation rates averaging 1.5–2.5 mm/day[38,40]. Rapid sedimentation in the foreland basin setting (up to 340 m/Ma)[31,39] resulted in a high-fidelity and high-temporal resolution record of fluvial processes across a c. 4 myr time period[34,36,39].

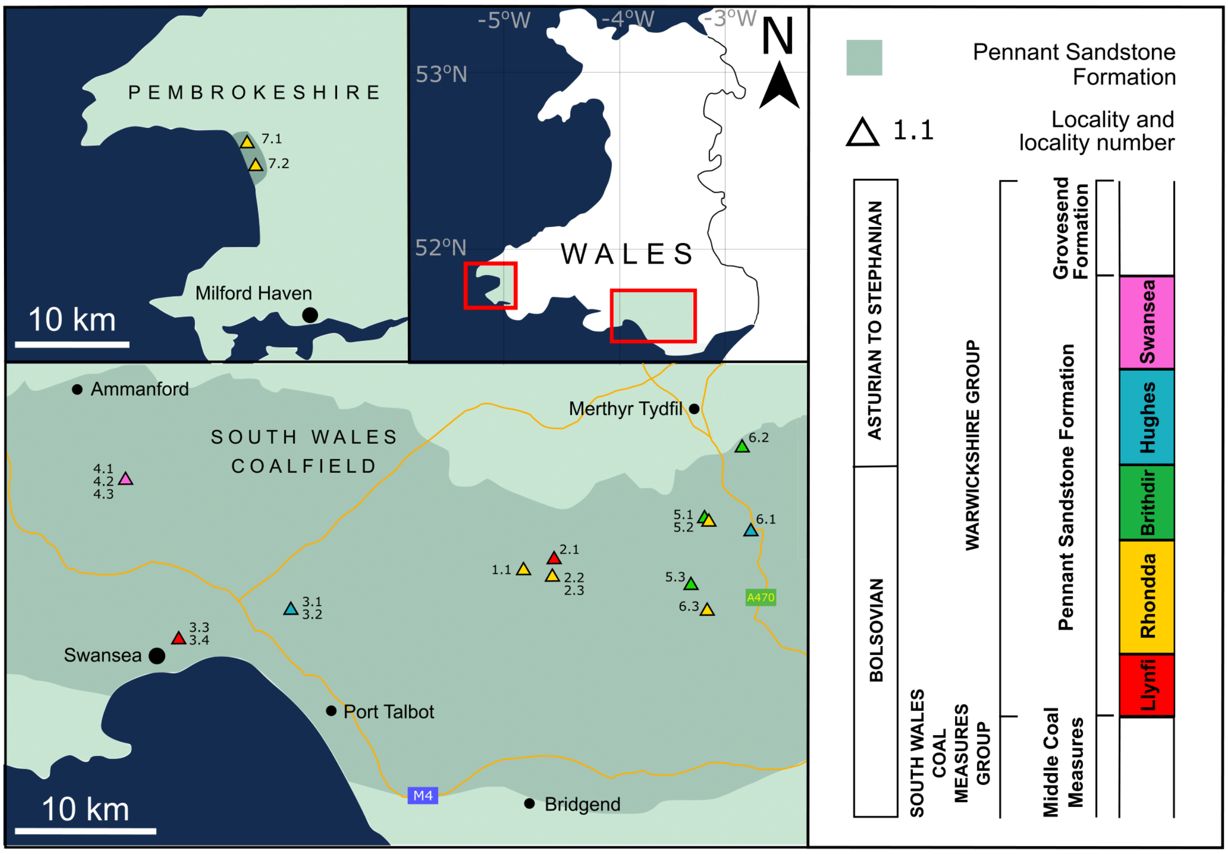

Figure 2: The South Wales and Pembrokeshire Coalfields, and the localities used for primary data collection. Pennant Formation geology is outlined after Jones and Hartley[34]. The stratigraphic column shows the five Members of the Pennant Formation, modified from Waters et al[35], and the localities are colour-coded by Member.

The formation comprises bedded, channelised sandstone bodies, with well-preserved accretion sets and abundant dune-scale cross-bedding[31]. Separating cliff-forming sandstone bodies are slope-forming fine-grained sediments representing floodplain deposition. They contain abundant and well-documented coals[39,41] indicating river migration across a forested, swampy foreland, characterised by high surface runoff and/or shallow water tables. These characteristics are consistent with meandering or anastomosing rivers which have been interpreted as showing perennial discharge regimes[19,31,34,36,39,41,42]. Qualitative observations of heterolithic deposits at channel margins (Fig. S5) representing crevasse splay deposits, and the presence of in-channel plant debris strongly point to the occurrence of flood events[39,43], some of which entrained flood plain vegetation[34,36,39]. These observations are consistent with the hypothesis in the thesis of Jones[39], based on extensive facies analysis across South Wales, that the Pennant Formation may have experienced variable discharge conditions. We therefore exploit this setting, as well as recent reconstructions of palaeo-rivers within the

Pennant Formation[31] to compare qualitative and quantitative evidence of disequilibrium flow conditions related to floods, and in doing so, quantify discharge variability in a Carboniferous river system for the first time.

3 Results

3.1 Fluvial facies and sedimentology

We first focus on the strong evidence of facies associations that can be robustly linked to floods before turning our attention to quantitative reconstructions. We identified two distinct facies associations in which woody debris occurs in great proportions: “Facies Association 1 (FA1)” observed in 15 locations across 7 localities, and “Facies Association 2 (FA2)” observed at 6 locations across 6 localities, although we stress that plant debris occurs ubiquitously throughout the formation (Fig. 3).

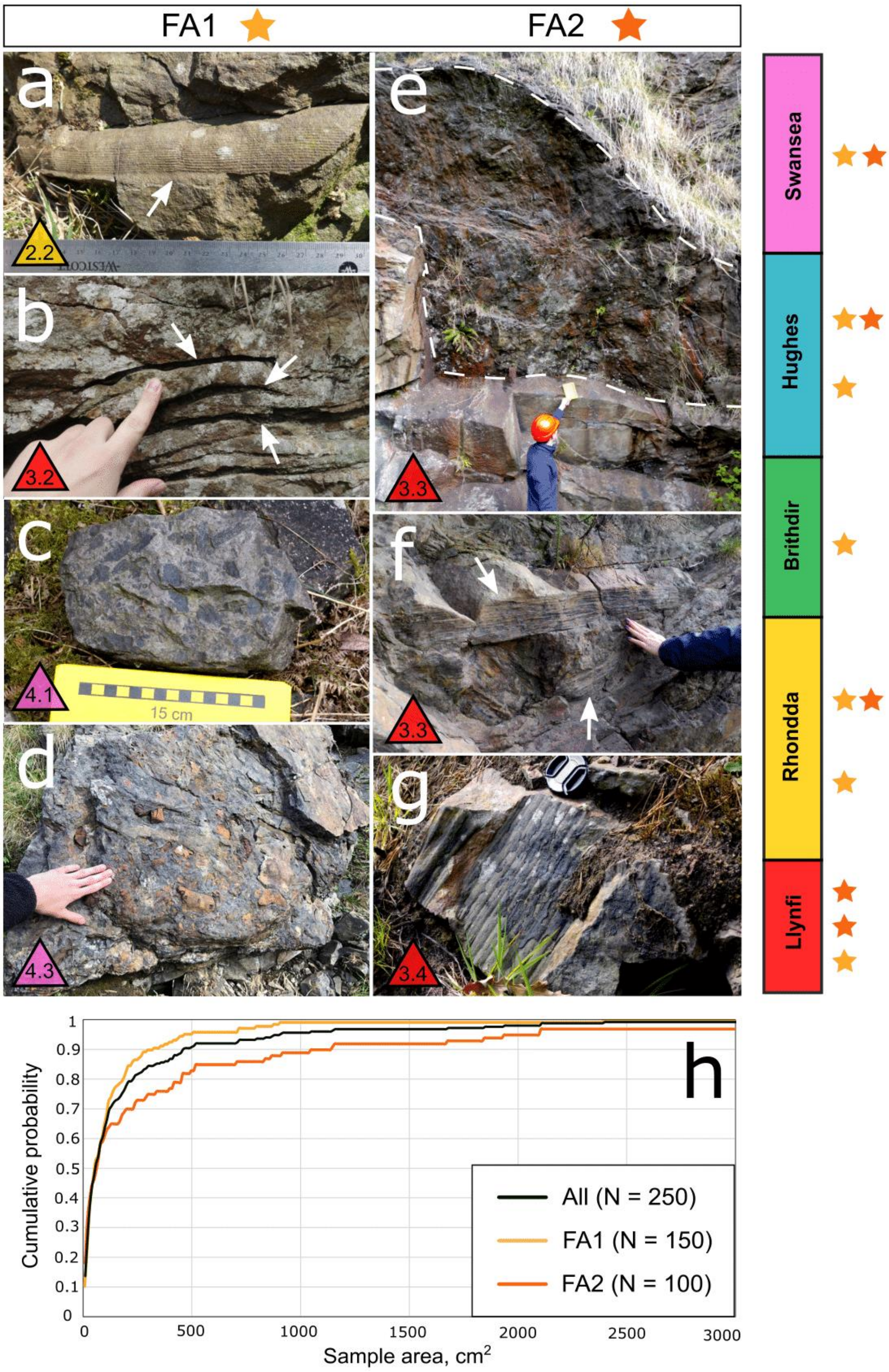

Figure 3: Facies-based evidence of flood-controlled deposition. (a-d) Facies Association 1: (a) well-preserved inner cast of an Equisetales *Calamites* stem; (b) entrained filaments of coalified organic-rich histosol (peaty soil); (c) compression fossils of disarticulated plant material (leaves, branches, and stems) representing a mixture of woody and non-woody macroflora: Lepidodendrales (*Lepidodendron*), Equisetales (*Calamites*), and ferns; (d) casts and three-dimensional permineralized fossils of woody debris with preferred alignment. (e-g) Facies Association 2: (e) debris bed exposed along a bedding plane, with well-articulated, but compacted, woody debris (mostly Lepidodendrales identified to the genus *Lepidodendron*) up to 2 m in length; (f) close-up of *Lepidodendron* stems/branches with surface layers (i.e. bark/cortical tissue) abraided prior to fossilization; (g) *Lepidodendron* cast with more intact surface layer present showing faint impressions of leaf scars. (h) Cumulative probability distribution of the sizes of woody debris samples observed within the two facies associations.

Facies Association 1:

This facies association (Fig 3a-d) is characterized by fossilized woody debris within channel sandstone packages, containing high-angle dune-scale cross-stratification. Plant fossils are preserved as a mixture of coalified compactions, compressions, as casts with well-preserved surface features, and occasional permineralization. They are often concentrated along horizons near the base of channel and accretion packages, but are also observed as isolated samples, distributed throughout stratigraphy. Identifiable fossils are mostly genus *Calamites*, with *Lepidodendron*, and some rarer *Stigmaria.* Also observed are coalified organic-rich histosol (peaty soil) filaments (Fig. 3b) and other compacted plant debris including non-woody leaf material (Fig. 3c). *Calamites* is a genus of arborescent Equisetales (= horsetails) extant through the Carboniferous until the Mid-Permian, which grew in riparian settings, proximal to channels, often inhabiting levees and overhanging river channels[42]. The presence of *Calamites* in channel and bar deposits suggests that discharge events regularly reached bankfull. Lepidodendrales (scale trees) represented by both *Lepidodendron* and *Stigmaria* lived further from active channels[42] and were larger and substantially denser than *Calamites*. Their presence as in-channel debris implies flood events which surpassed bankfull depth in order to inundate the floodplain and return samples to the channel.

It is possible to resolve the characteristics of flood events based on the size-distributions of fossils in debris beds, and we can link these to absolute magnitudes of flood events reconstructed from preserved bedforms (section 2.2). The mean length of debris fossils in Facies 1 is 16 cm, with a mean length/width ratio of 3.4. The exposed fossil surface area documented in this facies association has a mean of 135 cm^2 (Fig. 3h), and assuming that the samples represent cross-sections of cylindrical samples, the mean debris volume is tentatively reconstructed as 1472 cm^3, with a total measured volume of 0.22 m^3 of woody debris from 150 samples across 7 localities. We estimate that on average, woody debris in FA1 comprises 7% of the total exposed rock.

Facies Association 2:

This striking facies association comprises beds dominated by woody debris. These beds are poorly sorted, with fossils chaotically oriented, and large (>1 m long) samples overlapping and interlocked (e.g. Fig. 3e) in a matrix of sandstone. Debris bed units are between 1 and 4 m in thickness, and exist at the bases of barforms, accompanied by abundant upper plane bed sub-parallel lamination and some lower flow regime cross-bedding, indicating high flow transport stages. The chaotic orientation and sorting of these debris beds is typical of storm event beds that occur when extreme precipitation causes high-energy flood discharges, which were clearly capable of recruiting large clasts from the river levees and floodplain[5,44,45].

Fossils identified in FA2 were mostly *Lepidodendron* preserved as compactions and casts at varied stages of surface degradation. Fig. 3f shows a large sample of *Lepidodendron* with the outer layers of bark and cortical tissue abraided prior to burial, whereas Fig. 3g shows an example where more outer layers are preserved. We estimate that on average, woody debris in FA2 comprises 77% of the total exposed rock, with mean fossil length of 14.5 cm and a maximum of 2.5 m. The mean exposed fossil surface area documented in our study sites is 342 cm^2, and the mean estimated volume of debris samples is 5200 cm^3. The length/width ratio is 3.9, 15% higher than Facies 1, implying debris samples are less fragmented. The total estimated volume of debris measured in FA2 from 100 samples is 0.46 m^3. Fig. 3h shows that woody debris observed in FA2 possesses a larger range in sample size with greater skew towards large samples than in FA1.

3.2 Quantitative Analysis of Flood Stratigraphy

The facies analysis above shows that deposition in palaeo-rivers of the Variscan Foreland was influenced by high magnitude discharge events which regularly inundated floodplains. We now consider whether this formation also contains quantitative evidence of disequilibrium bedform preservation, consistent with the flood hypothesis[9,16,27], and if so, what this implies about flood durations.

The mean cross-set height, h_{xs}, across the Pennant Formation was 0.12 m, with a median value of 0.12 m and a standard deviation of 0.06 m (Fig. 4a). Values of maximum height measured within each cross-set average 0.19 m. Two-tailed Kolmogorov-Smirnov (KS) tests show that the h_{xs} distributions of the Pennant Formation's five Members are similar with 99.9% confidence (S3h), and Fig. 4a shows that the distributions of mean h_{xs} follow a similar pattern across all members. This analysis indicates that measured samples of cross-sets have similar height distributions at member and formation level. Although woody debris is ubiquitous throughout the formation, cross-set heights specifically associated with FA1 and FA2 above are lower because the deposits are less organised and/or show upper plane bed stratification consistent with flow speeds too great to sustain dune bedforms.

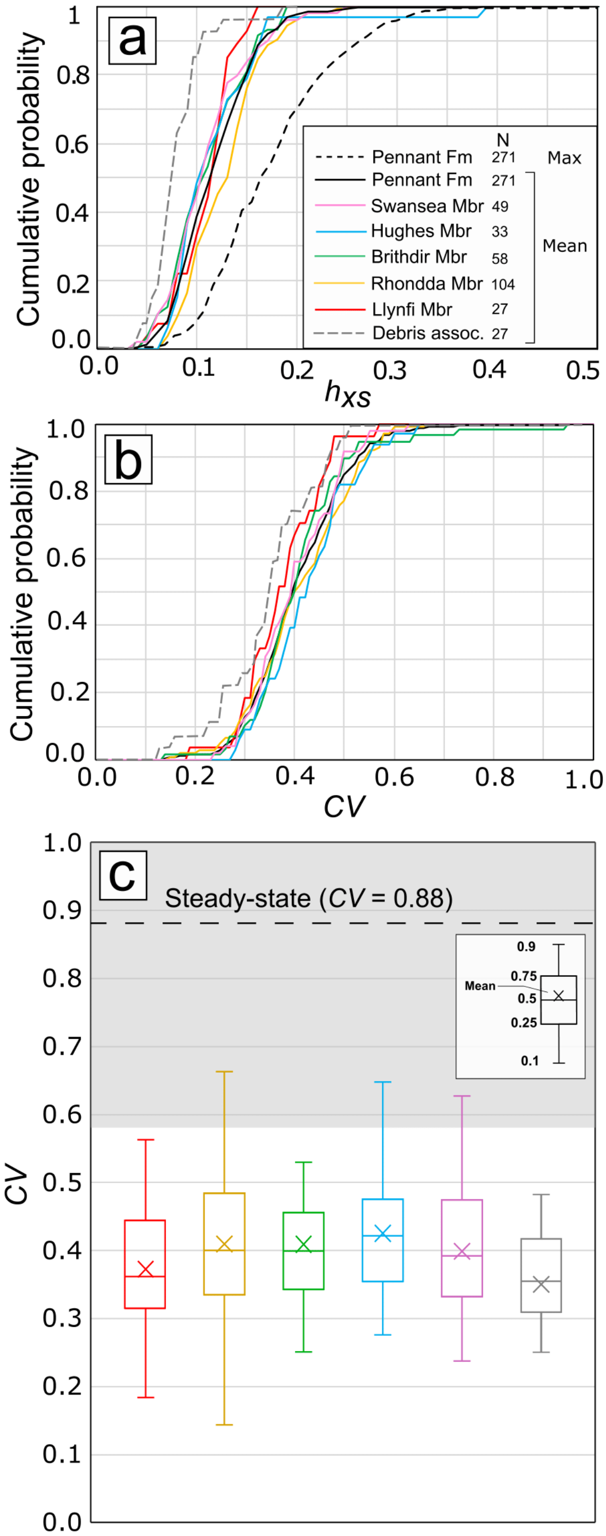

Figure 4: Cross-set data demonstrating disequilibrium bedform preservation. (a) Cumulative probability distributions of mean cross-set height for each Member of the Pennant Formation, with distributions of the mean, 84th percentile, maximum for the Pennant Formation overall, and cross-sets associated with woody debris; (b) similar to (a), but with distributions of *CV;* (c) the *CV* of each member of the Pennant Formation, with the width of each box proportional to the stratigraphic thickness of each Member measured near Swansea[46]. The dashed line and grey shaded region indicate the theoretical and empirical range of $CV(h_{xs})$ at steady state of 0.88 ± 0.3[24,25].

Results also show statistically similar low *CV* distributions for all members with 90% confidence with median *CV* values spanning 0.36–0.42 (Fig. 4b, Supplementary Information). The median for the Pennant Formation is 0.40 and the mean is 0.41. We emphasize that these *CV* values are significantly lower than the theoretical value expected for steady-state bedform preservation of $CV = 0.88 \pm 0.3$ (Fig. 4c)[16,24–26]. Indeed, 99.6% of cross-sets have *CV* below 0.88, and 96.7% have *CV* below 0.58 (0.88–0.3), suggesting that c. 97% of dunes measured were preserved in disequilibrium with the prevailing flow. These findings are consistent with theory and observations of disequilibrium (enhanced) bedform preservation[9,16,28,29], and come from a formation where there is very strong independent evidence for flood-dominated deposition[9,16] (Fig. 3). We stress that all members of the Pennant Formation show evidence of disequilibrium bedform preservation (Fig. 4c).

Furthermore, KS tests (see Methods and Supplementary Information) demonstrate that dune cross-sets observed in close association with woody debris have an even lower *CV* than those not associated with flood facies (Fig. 4b, c) with 90% confidence. This shows that, whilst bedform preservation for sandy channel deposits is enhanced consistently at formation level, an even greater enhancement is observed where debris-dominated flood facies are present. These data suggest that disequilibrium bedform preservation prevailed throughout the Pennant Formation and indicate a link between flood events and enhanced bedform preservation.

Significantly, these data can be used to quantify bedform turnover timescales, T_t, and prevailing flood duration, T_f. We first explore what our data imply assuming a minimum theoretical bedform preservation ratio (see Table 1) of 0.3[9,16,29] to obtain estimates of the maximum durations of T_t and T_t (Fig. 5A). Then we evaluate the sensitivity of these results to higher bedform preservation ratios.

T_t calculations (Eq. 3) suggest dunes required 3.2 days to be fully reworked by flow (Fig. 5B). Bedform theory and empirical observations[16] demonstrate dunes preserved in the falling limbs of flashy floods, in disequilibrium with the prevailing flow, have a bedform disequilibrium number, T^*, which represents the ratio of T_f and T_t, of < 1. When the *CV* of cross-set height is as low as 0.4, as our calculations show, T^* can be as low as 0.1[16]. This means given the average T_t of 3.2 days, T_f is reconstructed as c. 8 hours (0.32 days). Flashy floods often have almost symmetrical hydrographs[19], so the total length of the average flood preserved in the Pennant Formation can be approximated as 16 hours. To our knowledge this is the first time flood durations have been estimated for Carboniferous river systems. Based on paleohydrological calculations (Table 1 and Methods) we recover median bankfull discharges in individual channels as 140–160 m^3/s[31].

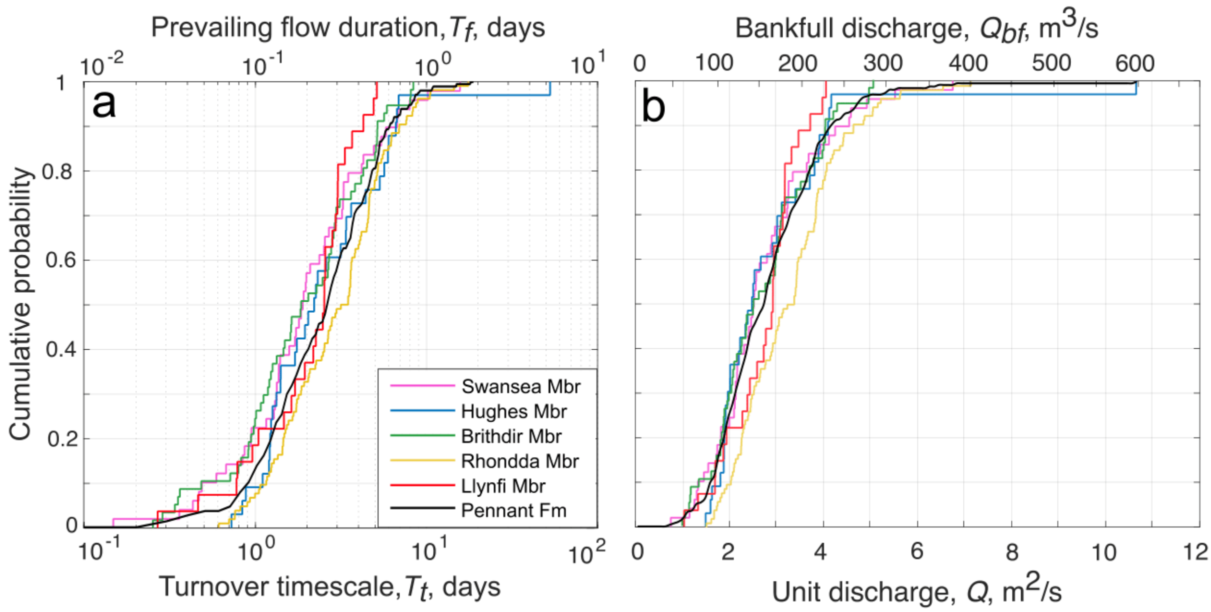

Figure 5: Cumulative probability distribution graphs showing key palaeohydrological variables. (a) The primary x-axis represents bedform turnover timescale, T_t, in each Member of the Pennant Formation, and the secondary x-axis indicates prevailing flow duration, T_f, which we set as $0.1T_t$, following Leary and Ganti[16]; (b) the primary x-axis represents the unit discharge, Q, and the secondary x-axis represents the bankfull discharge, Q_{bf}, calculated by multiplying Q by the average width of the channel, 55 m[31].

Because disequilibrium (enhanced) bedform preservation due to flooding is indicated by our *CV* values (Fig. 4), the estimates presented in Fig. 5a are conservative maxima[9]. The bedform preservation ratio, h_{xs}/h_d, is the ratio of measured mean cross-set height to estimated mean original dune height, and is influenced by the equilibrium dynamics of flow. Steady state dynamics are implicit in many bedform scaling relations[25], assuming $h_{xs}/h_d = 0.3$, however plausible non-steady state value of h_{xs}/h_d may be as great as 0.6, based on theory and experiments which show enhanced preservation during the falling limbs of flashy floods[9,16]. As h_{xs}/h_d increases from 0.3 to 0.6 for a known h_{xs} (0.12 m on average for the Pennant Formation), the median T_t reduces from 3.2 days to 0.9 days (Fig. 6A). This means that while the falling limb of floods may be as long as 8 hours assuming a 'typical' bedform preservation ratio of 0.3, T_f could be as short as 2.1 hours assuming a bedform preservation ratio as large as 0.6. Durations are very unlikely to be shorter than this as we do not see complete dunes preserved. The shaded regions in Fig. 6 illustrate the plausible range in palaeohydrologic parameters, with bankfull discharges for individual channels reconstructed from cross-set heights as between 88 and 160 m^3/s (Fig. 6B). Architectural constraints on channel morphology[31] result in comparable discharge reconstructions, with a median of 140 m^3/s per channel.

Finally, we note that the flow intermittency factor of a river, I_f, can be used to obtain quantitative context into annual flow regime, and can be visualised as the proportion of the year a river would need to maintain channel forming discharge conditions to equal an estimate of the yearly water budget. For ancient fluvial systems such as the Pennant Formation, I_f can be estimated using published constraints on palaeogeographic and palaeo-precipitation rates (see Methods) to obtain a plausible annual water budget, and we exploit these to obtain first-order intermittency estimates for Pennant rivers[39,41]. By comparing these constraints on mean annual discharge to our bankfull estimates (Fig. 6B), we estimate I_f = 0.17 – 0.44 (see Methods). This suggests that if the rivers of the Pennant Formation sustained bankfull conditions they could complete annual discharge in 62 – 160 days, which would be consistent with perennial river systems, as discussed further below.

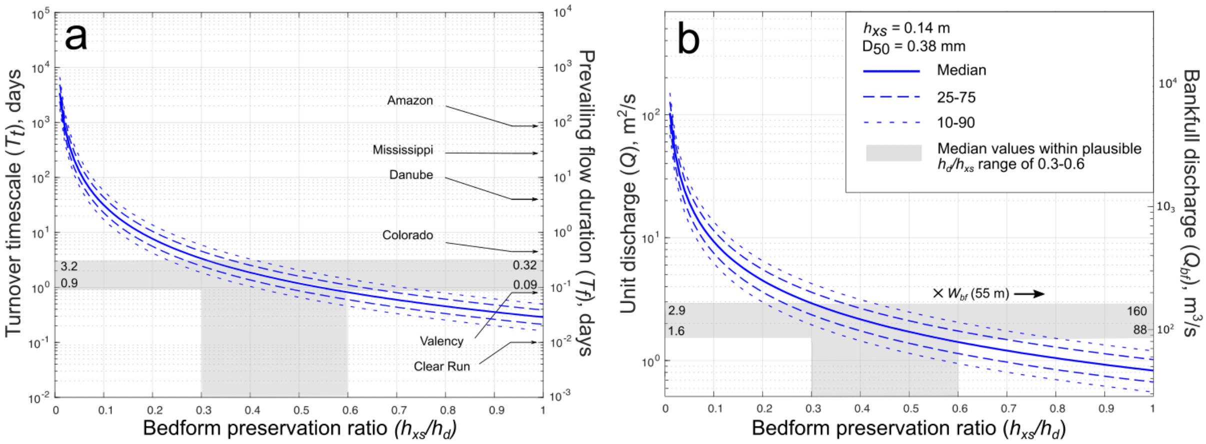

Figure 6: The effect of increased bedform preservation ratios on key palaeohydrologic parameters. (a) The primary y-axis indicates bedform turnover timescale, T_t, and the secondary y-axis indicates prevailing flow duration, T_f, when bedform disequilibrium number, T^*, is set as 0.1[16], and T_f of 6 modern rivers are given for comparison[28,47–51]; (b) the primary y-axis indicates unit discharge, Q, and the secondary y-axis indicates bankfull discharge, Q_{bf}, when channel width is set as 55 m, the average for the Pennant Formation[31].

4 Discussion

Bedform disequilibrium

Strong qualitative signals of flooding are ubiquitous in the Pennant Formation in the form of woody debris accumulations (Fig. 3) and overbank heterolithic packages (Supplementary Information), which outcrop in every member. In addition, we show that the abundance of flood facies across the formation is mirrored by the uniformity of enhanced bedform preservation, indicated by low coefficient of variation, CV of preserved dune cross-sets throughout the unit. The low cross-set CV of 0.4, across the formation, coupled with the clear evidence for variable discharge conditions demonstrates that stratigraphy in the Pennant Formation preserves non-steady-state bedform dynamics. We show that 97% of observed cross-sets (N = 271) possess low CV ($\leq 0.88 \pm 0.3$) consistent with enhanced dune preservation, and this appears to be the norm across up to 1.3 km of stratigraphy. This is the largest stratigraphic interval over which consistently enhanced bedform preservation has ever been documented, while facies observations of flood-controlled woody debris entrainment and deposition suggest that these disequilibrium conditions likely reflect the prevailing flow conditions during the falling limbs of floods. Short reconstructed falling limb flood durations (T_f) of 2–8 hours corroborate this interpretation, meaning that relatively flashy floods of total duration 4–16 hours, and with bankfull discharges of 140–160 m^3/s per channel thread were responsible for generating the bedforms observed.

Woody debris

We present two facies associations representing high densities of woody debris preserved throughout the Pennant Formation. The fossil size distributions (Fig. 3) and length/width ratios show that Facies Association 2 contains larger, longer debris samples. FA2 contains much higher density of debris, averaging 77% of outcrop, with chaotic orientation and organic preservation, whilst debris in FA1 are distributed sporadically and preserved mostly as casts. This implies the occurrence of two types of discharge events. The observation of large interlocking samples of debris suggests FA2 of the Pennant Formation represents log jam deposits[45], where the volume of wood entrained by flow was great enough to cause a dense raft of debris that saturated flow. These occur in extreme discharge events, with overbank flow high enough to entrain large stems and braches from the floodplain, with the potential to uproot and incorporate additional living plant material. Previous work also suggests that debris beds like these may be linked with channel avulsion events, and associated with avulsion-dominated systems[44]. Large woody debris and log-jam deposits have been documented in very similar tectono-climatic settings: Trümper et al[5] describe large woody debris in the Pennsylvanian Siebigerode Formation of central Germany, which they interpreted to represent high discharge recruitment of trunks and branches of Cordaitales and confiers from a vegetated lowland fluvial basin in the foreland of the Variscan Mountains c. 300 Ma. This shows that beds rich in debris may be typical of the Variscan Foreland in the Carboniferous, in addition to rivers associated high levels of flooding.

Where organic preservation occurs, particularly in FA2, it suggests burial was rapid, inhibiting the decomposition of organics. This is consistent with rapid sediment deposition expected of high magnitude discharge events[19], suggesting FA2 was formed during significant storm events. The higher-fidelity surface preservation of fossil casts in FA1 implies they were exposed to more limited abrasion, which we interpret to reflect transport in flow for only a short period of time prior to burial. This suggests many samples were detached and dead on the forest floor before they were recruited into the river, meaning they could be readily inundated by water, becoming dense enough to be rapidly deposited and buried on riverbeds before transport abrasion strongly reduced the fidelity of the fossil preservation. Conversely, well-preserved fossil exteriors, particularly in FA2, could also be attained by recruitment of recently unrooted vegetation to channelised flow, resulting in transported clasts that were more resistant to erosion and decomposition.

Not only are evidence of enhanced bedform preservation and facies evidence of flood variability both present across 1.3 km of stratigraphy, but our data are unique in demonstrating how the two can be quantitatively linked. While woody debris is ubiquitous throughout the Pennant Formation, where it is found in greater volumes (our Facies Associations 1 and 2) it coincides with lower cross-set *CV* to 90% confidence (Fig. 5b). While almost all cross-sets measured indicate disequilibrium preservation, interpreted to be driven by flashy floods, dunes shown to have occurred in stratigraphic proximity to debris-transporting flood events are preserved with the lowest *CV* values.

Consequently, we can confidently suggest a model of river flooding in this upper Carboniferous fluvial environment. Regular high-flow events reached at least bankfull depth, eroding the river banks and entraining fresh and dead plant material, mostly *Calamites,* into the channel from the levees and proximal floodplain. Less frequent, higher magnitude floods potentially caused by intense precipitation and possibly associated with channel avulsion, resulted in flow depths exceeding bankfull. Flow inundated the floodplain, recruiting large freshly uprooted samples of *Lepidodendron* and *Calamites* and buoying those loose on the forest floor. These were recruited to the channel during waning flow, and rapidly deposited along with high flow-regime bedforms, maintaining preservation of organics. This model is consistent with some established interpretations of the palaeoenvironment of the Pennant Formation[34,39], in addition to palaeohydrologic reconstructions[31] and studies of modern woody debris recruitment[53–56].

Facies-based evidence of both high and low-magnitude flooding, coupled with a quantitative bedform analysis of disequilibrium bedform dynamics depicts a realistic system that is affected by a range of discharge conditions and is consistent with bedform-derived interpretations of disequilibrium flow. This shows that woody debris and low cross-set *CV* are robust indicators of flood discharge in palaeo-rivers, and highlights the critical importance of uniting facies-based evidence of variable discharge conditions with quantitative insights from bedform theory.

Discharge regimes

Facies evidence indicates that rivers were perennial rather than ephemeral[13,19,20,31,34,39]: Plink-Bjorklund[19] presents indicators to identify ephemeral and monsoonal systems in the geologic record, including Froude transcritical or supercritical structures, such as antidune laminae, and evidence of long periods free of discharge, such as *in-situ* vegetation. In these deposits trans- or supercritical sedimentary structures have been rarely observed. Furthermore, whilst we observed well-preserved plant debris within channel deposits, we did not observe plant fossils *in-situ*, e.g. intact stems situated within the channel, meaning we cannot infer that plants were able to colonise the river channel during dry seasons. The fact that the only fossil plants observed are abundant fluvially transported debris suggests the rivers were not subject to extreme seasonality[20,57,58]. Furthermore, we and others have observed well-developed accretion sets, characteristic of perennial river deposits, as opposed to streams supplied largely by seasonal precipitation[19,21,22,59–62]. Serinaldi et al[47] also note that monsoonal regimes are typically characterized by sustained floods (5–25 days), whereas perennial river floods have shorter durations. T_t calculations yield flood durations less than 1 day, which would be inconsistent with models of subtropical systems, but consistent with precipitation (storm) driven floods in a perennial system. Additionally, Leary and Ganti[16] found that sustained floods may have sufficiently long flood recessions such that bedforms reach equilibrium with the flow, in contrast with our results showing disequilibrium bedform preservation.

It is also significant that the water flux intermittency factor, I_f, obtained for the Pennant Formation of 0.17 to 0.44 is not consistent with ephemeral discharge rivers[9,30] but can be directly compared with systems today such as the Mississippi River, USA, with $I_f = 0.3$[49] and the Minnesota River, USA, with $I_f = 0.175$[63]. These are both characterized by high precipitation rates of 900 mm/a (2.5 mm/day)[64] and 700 mm/a (2 mm/day)[65], respectively, similar to those expected of Carboniferous Wales[38]. Consequently, the intermittency factors we obtain are broadly characteristic of perennial flow in sand-bedded rivers documented in modern humid environments[33].

Stratigraphic completeness

One implication of the low CV values for fluvial cross-sets documented in this study is that they imply elevated bedform preservation ratios. Consequently, the palaeohydrological and facies-based results of this study show the unusual completeness[14] of the strata (in terms of bedform preservation) is likely due to discharge variability related to flooding[16,19,31]. This conclusion raises important questions about preservation of flow events in the stratigraphic record[14,24]. Variscan tectonics and associated accommodation generation clearly contributed to the high rates of fluvial deposition, as well as the preservation of woody debris[5]. However, given that almost the entire stratigraphic record of the Pennant contains the signature of disequilibrium bedform preservation, steady-state flow conditions appear to be very poorly preserved in the stratigraphic archive studied here. One explanation might be that rivers may evolve in a state of disequilibrium with the prevailing flow most of the time[e.g., 15]. This would be due to the known hysteresis[68] between flow conditions and adjusting dune morphology. If this is true for the Pennant Formation, then this study offers the best documented evidence that ancient rivers should not be treated as binary – either at steady-state or non-steady-state – but that disequilibrium bedform preservation is occurring regularly due to low-level discharge variability.

However, given that we have extensive facies-based evidence for flood discharge conditions, our observations (e.g. Fig. 3) provide clear evidence for significant changes in flow conditions. Consequently, floods occurred relatively briefly, as we quantify above, leaving perennial flow states to dominate the annual hydrograph, but not the sedimentary record. In this scenario, the finding that 97% of observed cross-sets show *CV* values inconsistent with steady-state bedform preservation as a result of flood-driven discharge variability would imply that the vast majority of geologic time has been excluded from the depositional record[14]. This study shows that disequilibrium flow conditions driven by flooding may be ubiquitous but under-recognized in the geologic record. Therefore, our data analysis also provides a new route to quantify preservation bias in the stratigraphic archive.

Taken together, these results demonstrate vividly how a careful combination of bedform and facies-based approaches can unlock fresh insights into Earth's sedimentary systems. This study represents the first quantitative investigation of bedform dynamics in upper Carboniferous palaeo-rivers and demonstrates how preserved bedforms can be used to extract signals of ancient discharge variability from fluvial stratigraphy. We show that the rivers in the Variscan foreland of the UK were significantly influenced by flood variability, the signature of which dominated stratigraphy over a period of 4 Ma. Palaeo-rivers had flow intermittencies of 0.17-0.44, consistent with precipitation- (storm-) driven flooding in a sand-bedded perennial river regime. Floods had duration 4–16 hours, causing enhanced preservation of dunes and recruiting large quantities of woody debris, sometimes in the form of log jams, and flood discharges had magnitudes of 140–160 m^3/s for individual channel threads.

5 Methods

5.1 Field observations

Primary data were collected in Autumn 2021 and Spring 2022 across 19 sites in the South Wales and Pembrokeshire Coalfields (Figure 2; Supplementary Information) from the five Members of the Pennant Formation. Primary data included cross-set heights (Fig. 8a, b), grain-size (Fig. 8e, f), the geometries of various architectural elements (Fig. 8c, d), and observations of flood facies (Fig. 3).

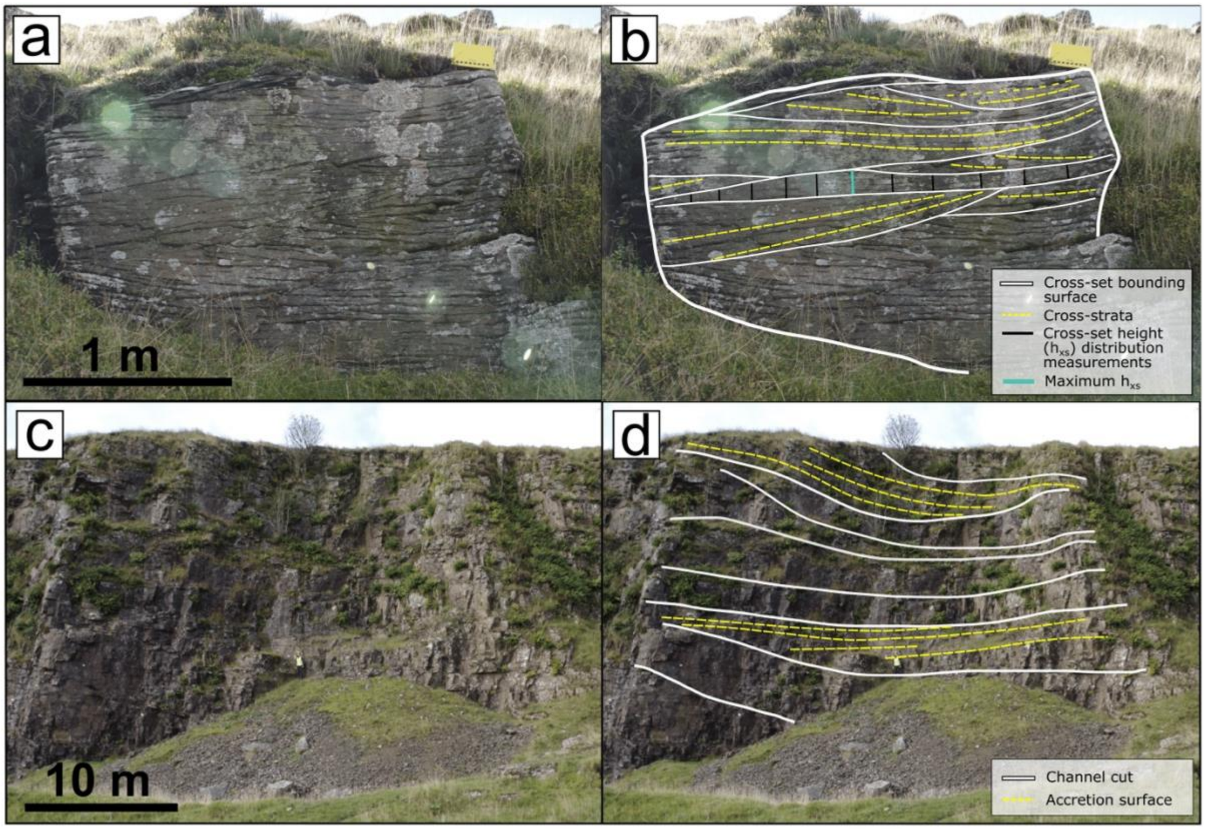

Fig. 8: Field measurements and methodology. (a, b) Methods of collecting cross-set height measurements, where the vertical bars make one cross-set height distribution, Locality 6.2; (c, d) architectural elements observed at outcrop scale, including accretion surfaces for use in Equation 7, Locality 2.1.

Cross-set heights were collected following the sampling strategy of Lyster et al[9], Ganti et al[27] and Wood et al[31] with methods outlined in Fig. 8b. Cross-set bounding surfaces were first identified, and cross-set height was measured (to a precision of ± 5 mm) perpendicular to its long-axis at regular intervals, with between 7 and 61 measurements per cross-set. A total of 4390 height measurements were taken across 271 cross-sets (S3b). Measurements of maximum cross-set height (with sample size N = 1735) were also collected separately. Relationships were established between the maximum and mean height from the recorded distributions (Supplementary Information), allowing estimation of mean h_{xs} from cross-sets where only the maximum value was measured. This increased the sample size of mean cross-set heights to N = 6125.

For each observed cross-set, the grain-size of the sediment was also established. Most cross-sets were preserved in sand-grade deposits, but we also observed rare pebble-grade cross-sets. The grain-size of sand-fractions (<2 mm) was estimated in the field according to size terms of the Wentworth[69] classification, confirmed by processing of grain-size images in ImageJ software, and the median grain-size (D_{50}) was extracted. The geometries of architectural elements were measured using a Haglof Laser Geo laser range finder to a precision of ± 5 cm. These included the dimensions of channel and accretion packages.

5.2 Quantitative palaeohydrology

Fundamental to the "flood hypothesis"[29] is the detection of enhanced bedform preservation in fluvial strata. Measured h_{xs} distributions were used to calculate the coefficient of variation of cross-set height, *CV,* where:

$$CV = \frac{\sigma}{\mu}$$

Eq. 1

in which σ is the standard deviation and μ is the mean of the cross-set heights within a single cross-set. The *CV* reflects the preservation of the original dune, and therefore the equilibrium dynamics of flow: a *CV* of 0.88 is expected in equilibrium conditions[24–26] and *CV* decreases as bedform preservation becomes enhanced (Fig. 1).

To calculate the original dune height from cross-sets observed in the field, the relationship established by Leclair and Bridge [25] was used, based on previous theoretical work[24]:

$$h_d = 2.9(\pm 0.7)h_{xs}$$

Eq. 2

where h_d is the mean original dune height, and h_{xs} is the mean cross-set height. Values of h_d were then used in an array of further palaeohydrological calculations to build a complete picture of river morphodynamics (see Supplementary Information 4, 'Extended methodology' and Wood et al[31]). This relationship implies a bedform preservation ratio of 0.3, which assumes bedforms were preserved in equilibrium with flow, so uncertainty has been plotted in Fig. 5.

To estimate uncertainty, Monte Carlo uncertainty propagation was used to generate a distribution of values for h_d that reflects the true spread of the data, as has been done successfully in previous hydrological studies[9,30,32]. For Equation 2, 10^6 random samples were generated between bounds defined by $\mu - \sigma$ and $\mu + \sigma$ where μ is the mean and σ is one standard deviation. This was repeated for all formulae with a stated error, and propagated uncertainties were carried through.

Bedform turnover timescale (T_t) is defined as the time to displace the volume per unit width of sediment in a bedform, i.e., the length of time required for a bedform to be completely reworked by the prevailing flow[15]. This parameter is used to indicate whether bedforms evolved in equilibrium with the prevailing flow, as a T_t that is greater than the duration of the prevailing flow, T_f, implies a hysteresis that results in limited reworking of the bedform. This study determines T_t using the methods of Myrow et al[15] and Martin and Jerolmack[68], in which:

$$T_t = \frac{\lambda h_d \beta}{q_b}$$

Eq. 3

where λ is dune wavelength (approximated as $\lambda = 7.3H$, where H is the formative flow depth), the shape factor $\beta \approx 0.55$ and q_b is the unit bedload flux (Extended Methodology Eq. 9). Myrow et al[15] define a dimensionless bedform disequilibrium number, T^*:

$$T* = \frac{T_f}{T_t}$$

Eq. 4

Using data compiled from experiments and modern rivers by Leary and Ganti[16], it is possible to establish plausible values of T^* for calculated values of CV. Their results imply that dunes preserved in disequilibrium with falling-limb flood discharge lead to cross-sets low values of CV and T^*. Based on their data, we take 0.1 as a plausible value of T^*, meaning $T_f = 0.1T_t$.

The flow intermittency factor, I_f, is defined as the fraction of the total time in which bankfull flow would accomplish the same amount of water discharge as the real hydrograph[33]:

$$I_f = \frac{\Sigma\, Q(t)}{Q_{bf}\, \Sigma\, t}$$

Eq. 5

where ΣQ(t) is the sum of the time dependent discharge (i.e., the unit discharge), Q_{bf} is the discharge at bankfull conditions and Σt is the timespan. Flow intermittency requires estimation of a yearly water budget, and this necessitates a range of assumptions. Based on atmospheric general circulation models[38,40], the palaeo-precipitation rate was estimated as between 1.5 and 2.5 mm/day (0.55 - 0.91 m/yr), and catchment area has been estimated by Wood et al[31] as 4500 - 9500 km^2, based on catchment scaling relationships[70] and previously published palaeogeographic constraints[37]. Multiplying the annual average precipitation rate by the catchment area gives an estimate of the discharge (m^2/s) supplied to the catchment, once modified to account for infiltration[71].

5.3 Statistical tests

Two-tailed Kolomogorov-Smirnov (KS) tests were performed in order to test the similarity of datasets, with the null hypothesis that the tested datasets have similar distributions. Firstly, the h_{xs} data collected in each member were tested against each other and against the data collected from the Pennant Formation as a whole. Secondly, the same tests were conducted for the cross set *CV*. Finally, the *CV* values of cross-sets associated with woody debris were tested against those not associated with debris. See S3h, S3i and S3j, respectively, for these statistical tests.

Acknowledgements

The authors acknowledge research support from Imperial College London. We thank Gary Hampson and Cedric John for useful feedback on an early version of the manuscript.

Author contributions

JSM: Data curation (lead), formal analysis (lead), investigation (lead), methodology (lead), visualization (lead), visualisation (lead), writing – original draft (lead), writing – review and editing (equal); **JW:** Data curation (supporting), formal analysis (supporting), investigation (supporting), methodology (supporting), writing – review and editing (equal); **SJL**: Data curation (supporting), formal analysis (supporting), investigation (supporting), methodology (supporting), supervision (equal), writing – review and editing (equal); **JV**: Formal analysis (supporting) investigation (supporting), methodology (supporting), writing – review and editing (supporting); **ARTS:** Formal analysis (supporting), investigation (supporting), writing

– review and editing (supporting); **ACW**: Data curation (supporting), formal analysis (supporting), investigation (supporting), methodology (supporting), supervision (equal), writing – review and editing (equal).

Competing interests

The authors declare no competing interests.

Supplementary information

S1: Table of localities

S2: Localities and access (.kmz)

S3: Field data and statistical analysis

S4: Extended methodology

S5: Sedimentary Logs of crevasse splay deposits at Locality 4.3

References

1. Milliman, J. D. & Meade, R. H. Worldwide delivery of river sediment to the oceans. *Geology* **91**, 1–21 (1983).
2. Ben-Israel, M., Armon, M., ASTER & Matmon, A. Sediment residence times in large rivers quantified using a cosmogenic nuclides based transport model and implications for buffering of continental erosion signals. *J Geophys Res Earth Surf* **127**, (2022).
3. Baker, V. R., Kochel, R. C. & Patton, P. C. *Flood Geomorphology*. (Wiley-Interscience, 1988).
4. Parsons, M., McLoughlin, C. A., Kotschy, K. A., Rogers, K. H. & Rountree, M. W. The effects of extreme floods on the biophysical heterogeneity of river landscapes. *Frontiers in Ecology and the Environment* **3**, 487–494 (2009).
5. Trümper, S. *et al.* Late Palaeozoic red beds elucidate fluvial architectures preserving large woody debris in the seasonal tropics of central Pangaea. *Sedimentology* **67**, 1973–2012 (2020).
6. Hering, D., Gerhard, M., Manderbach, R. & Reich, M. Impact of a 100-year flood on vegetation, benthic invertebrates, riparian fauna and large woody debris standing stock in an alpine floodplain. *River Res Appl* **20**, 445–457 (2004).
7. Palik, B. *et al.* Geomorphic variation in riparian tree mortality and stream coarse woody debris recruitment from record flooding in a coastal plain stream. *Écoscience* **5**, 551–560 (2016).

8. Comiti, F., Lucía, A. & Rickenmann, D. Large wood recruitment and transport during large floods: A review. *Geomorphology* **269**, 23–39 (2016).
9. Lyster, S. J., Whittaker, A. C., Hajek, E. A. & Ganti, V. Field evidence for disequilibrium dynamics in preserved fluvial cross-strata: A record of discharge variability or morphodynamic hierarchy? *Earth Planet Sci Lett* **579**, (2022).
10. Whittaker, A. C. *et al.* Flood variability in the rock record? Disequilibrium bedform preservation in ancient fluvial stratigraphy. in *EGU General Assembly, Vienna, Austria, 23-27 May 2022, EGU-6440* (2022).
11. Watkins, S. E. *et al.* Are landscapes buffered to high-frequency climate change? A comparison of sediment fluxes and depositional volumes in the Corinth Rift, central Greece, over the past 130 k.y. *GSA Bulletin* **131**, 372–388 (2018).
12. Romans, B. W., Castelltort, S., Covault, J. A., Fildani, A. & Walsh, J. P. Environmental signal propagation in sedimentary systems across timescales. *Earth Sci Rev* **153**, 7–29 (2016).
13. Fielding, C. R., Alexander, J. & Allen, J. P. The role of discharge variability in the formation and preservation of alluvial sediment bodies. *Sediment Geol* **365**, 1–20 (2018).
14. Paola, C., Ganti, V., Mohrig, D., Runkel, A. C. & Straub, K. M. Time Not Our Time: Physical Controls on the Preservation and Measurement of Geologic Time. *Annual Review of Earth and Planetary Sciences* **46**, 409–438 (2018).
15. Myrow, P. M., Jerolmack, D. J. & Perron, J. T. Bedform disequilibrium. *Journal of Sedimentary Research* **88**, 1096–1113 (2018).
16. Leary, K. C. P. & Ganti, V. Preserved Fluvial Cross Strata Record Bedform Disequilibrium Dynamics. *Geophys Res Lett* **47**, (2020).
17. Foreman, B. Z., Heller, P. L. & Clementz, M. T. Fluvial response to abrupt global warming at the Palaeocene/Eocene boundary. *Nature* **491**, 92–95 (2012).
18. Colombera, L., Arévalo, O. J. & Mountney, N. P. Fluvial-system response to climate change: The Paleocene-Eocene Tremp Group, Pyrenees, Spain. *Glob Planet Change* **157**, 1–17 (2017).
19. Plink-Björklund, P. Morphodynamics of rivers strongly affected by monsoon precipitation: Review of depositional style and forcing factors. *Sediment Geol* **323**, 110–147 (2015).
20. Fielding, C. R., Allen, J. P., Alexander, J. & Gibling, M. G. Facies model for fluvial systems in the seasonal tropics and subtropics. *Geology* **37**, 623–626 (2009).
21. Adams, M. M. & Bhattacharya, J. P. No change in fluvial style across a sequence boundary, Cretaceous Blackhawk and Castlegate formations of central Utah, U.S.A. *Journal of Sedimentary Research* **75**, 1038–1051 (2005).
22. Chamberlin, E. P. & Hajek, E. A. Using bar preservation to constrain reworking in channel-dominated fluvial stratigraphy. *Geology* **47**, 531–534 (2019).
23. McMahon, W. J. & Davies, N. S. High-energy flood events recorded in the Mesoproterozoic Meall Dearg Formation, NW Scotland; their recognition and implications for the study of pre-vegetation alluvium. *J Geol Soc London* **175**, 13–32 (2018).
24. Paola, C. & Borgman, L. Reconstructing random topography from preserved stratification. *Sedimentology* **38**, 553–565 (1991).
25. Leclair, S. F. & Bridge, J. S. Quantitative interpretation of sedimentary structures formed by river dunes. *Journal of Sedimentary Research* **71**, 713–716 (2001).
26. Leclair, S. F. Preservation of cross-strata due to the migration of subaqueous dunes: an experimental investigation. *Sedimentology* **49**, 1157–1180 (2002).

27. Ganti, V., Whittaker, A. C., Lamb, M. P. & Fischer, W. W. Low-gradient, single-threaded rivers prior to greening of the continents. **116**, 11652–11657 (2019).
28. Leary, K. & Buscombe, D. Estimating Sand Bedload in Rivers by Tracking Dunes: a comparison of methods based on bed elevation time-series. *Earth Surface Dynamics Discussions* **8**, 161–172 (2019).
29. Ganti, V., Hajek, E. A., Leary, K., Straub, K. M. & Paola, C. Morphodynamic Hierarchy and the Fabric of the Sedimentary Record. *Geophys Res Lett* **47**, (2020).
30. Lyster, S. J. *et al.* Reconstructing the morphologies and hydrodynamics of ancient rivers from source to sink: Cretaceous Western Interior Basin, Utah, USA. *Sedimentology* **68**, 2854–2886 (2021).
31. Wood, J., McLeod, J. S., Lyster, S. J. & Whittaker, A. C. Rivers of the Variscan Foreland: fluvial morphodynamics in the Pennant Formation of South Wales, UK. *Journal of the Geological Society* (2022) doi:https://doi.org/10.31223/X5TK94.
32. Mahon, R. C. & McElroy, B. Indirect estimation of bedload flux from modern sand-bed rivers and ancient fluvial strata. *Geology* **46**, 579–582 (2018).
33. Hayden, A. T., Lamb, M. P. & McElroy, B. J. Constraining the Timespan of Fluvial Activity From the Intermittency of Sediment Transport on Earth and Mars. *Geophys Res Lett* **48**, (2021).
34. Jones, J. A. & Hartley, A. J. Reservoir characteristics of a braid-plain depositional system: the Upper Carboniferous Pennant Sandstone of South Wales. *Geological Society Special Publications* **73**, 143–156 (1993).
35. Waters, C. N., Waters, R. A., Barclay, W. J. & Davies, J. R. *A lithostratigraphical framework for the Carboniferous successions of southern Great Britain (onshore)*. (2009).
36. Falcon-Lang, H. J., Cleal, C. J., Pendleton, J. L. & Wellman, C. H. Pennsylvanian (mid/late Bolsovian-Asturian) permineralised plant assemblages of the Pennant Sandstone Formation of southern Britain: Systematics and palaeoecology. *Rev Palaeobot Palynol* **173**, 23–45 (2012).
37. Burgess, P. M. & Gayer, R. A. Late Carboniferous tectonic subsidence in South Wales: implications for Variscan basin evolution and tectonic history in SW Britain. *J Geol Soc London* **157**, 93–104 (2000).
38. Tabor, N. J. & Poulsen, C. J. Palaeoclimate across the Late Pennsylvanian-Early Permian tropical palaeolatitudes: A review of climate indicators, their distribution, and relation to palaeophysiographic climate factors. *Palaeogeogr Palaeoclimatol Palaeoecol* **268**, 293–310 (2008).
39. Jones, C. M. The sedimentology of Carboniferous fluvial and deltaic sequences; the Roaches Grit Group of the South-West Pennines and the Pennant Sandstone of the Rhondda Valleys. (Keele University, 1977).
40. Peyser, C. E. & Poulsen, C. J. Controls on Permo-Carboniferous precipitation over tropical Pangaea: A GCM sensitivity study. *Palaeogeogr Palaeoclimatol Palaeoecol* **268**, 181–192 (2008).
41. Jenkins, B. H. J. The sequence and correlation of the coal measures of Pembrokeshire. *Quarterly Journal of the Geological Society* **118**, 65–101 (1961).
42. Cleal, C. J. & Thomas, B. M. *Plant fossils of the British Coal Measures*. (The Palaeontological Association, 1994).
43. van Toorenenburg, K. A., Donselaar, M. E. & Weltje, G. J. The life cycle of crevasse splays as a key mechanism in the aggradation of alluvial ridges and river avulsion. *Earth Surf Process Landf* **43**, 2409–2420 (2018).
44. Edmonds, D. A. *et al.* Rivers in reverse: Upstream-migrating dechannelization and flooding cause avulsions on fluvial fans. *Geology* **50**, 37–42 (2021).

45. Davies, N. S. & Gibling, M. R. The sedimentary record of Carboniferous rivers: Continuing influence of land plant evolution on alluvial processes and Palaeozoic ecosystems. *Earth Sci Rev* **120**, 40–79 (2013).
46. Bedrock map of Swansea, Geological Survey of England and Wales 1:50,000 geological map series, New Series Sheet 247. *British Geological Survey* (2011).
47. Serinaldi, F., Loecker, F., Kilsby, C. G. & Bast, H. Flood propagation and duration in large river basins: a data-driven analysis for reinsurance purposes. *Natural Hazards* **94**, 71–92 (2018).
48. Musolino, G. & Ahmadian, R. A new approach in the design of evacuation/access routes using a fully conservative 2D model. in *38th IAHR World Congress - 'Water: Connecting the World'* vol. 38 4144–4155 (The International Association for Hydro-Environment Engineering and Research, 2019).
49. Nittrouer, J. A., Allison, M. A. & Campanella, R. Bedform transport rates for the lowermost Mississippi River. *J Geophys Res Earth Surf* **113**, (2008).
50. Sukhodolov, A. N., Fedele, J. J. & Rhoads, B. L. Structure of flow over alluvial bedforms: An experiment on linking field and laboratory methods. *Earth Surf Process Landf* **31**, 1292–1310 (2006).
51. Almeida, R. P. de *et al.* Large barchanoid dunes in the Amazon River and the rock record: Implications for interpreting large river systems. *Earth Planet Sci Lett* **454**, 92–102 (2016).
52. Bradley, R. W. & Venditti, J. G. Reevaluating dune scaling relations. *Earth Sci Rev* **165**, 356–376 (2017).
53. Golladay, S. W., Battle, J. M. & Palik, B. J. Large wood debris recruitment on differing riparian landforms along a Gulf Coastal Plain (USA) stream: A comparison of large floods and average flows. *River Res Appl* **23**, 391–405 (2007).
54. Gurnell, A. M., Piégay, H., Swanson, F. J. & Gregory, S. v. Large wood and fluvial processes. *Freshw Biol* **47**, 601–619 (2002).
55. Gurnell, A. M. Wood in Fluvial Systems. in *Treatise on Geomorphology* vol. 9 163–188 (Elsevier Inc., 2013).
56. Moulin, B., Schenk, E. R. & Hupp, C. R. Distribution and characterization of in-channel large wood in relation to geomorphic patterns on a low-gradient river. *Earth Surf Process Landf* **36**, 1137–1151 (2011).
57. Allen, J. P., Fielding, C. R., Rygel, M. C. & Gibling, M. R. Deconvolving signals of tectonic and climatic controls from continental basins: An example from the late paleozoic Cumberland Basin, Atlantic Canada. *Journal of Sedimentary Research* **83**, 847–872 (2013).
58. Allen, J. P., Fielding, C. R., Gibling, M. R. & Rygel, M. C. Recognizing products of palaeoclimate fluctuation in the fluvial stratigraphic record: An example from the Pennsylvanian to Lower Permian of Cape Breton Island, Nova Scotia. *Sedimentology* **61**, 1332–1381 (2014).
59. Cotter, E. Paleoflow characteristics of a late Cretaceous river in Utah from analysis of sedimentary structures in the Ferron Sandstone. *J Sediment Petrol* **41**, 129–142 (1971).
60. Miall, A. D. Reconstructing fluvial macroform architecture from two-dimensional outcrops: examples from the Castlegate Sandstone, Book Cliffs, Utah. *Journal of Sedimentary Research* **B64**, 146–158 (1994).
61. Hampson, G. J., Jewell, T. O., Irfan, N., Gani, M. R. & Bracken, B. Modest change in fluvial style with varying accommodation in regressive alluvial-to-coastal-plain wedge: Upper Cretaceous Blackhawk Formation, Wasatch Plateau, central Utah, U.S.A. *Journal of Sedimentary Research* **83**, 145–169 (2013).

62. Flood, Y. S. & Hampson, G. J. Facies and architectural analysis to interpret avulsion style and variability: Upper Cretaceous Blackhawk Formation, Wasatch Plateau, Central Utah, U.S.A. *Journal of Sedimentary Research* **84**, 743–762 (2014).
63. Czuba, J. A. & Foufoula-Georgiou, E. A network-based framework for identifying potential synchronizations and amplifications of sediment delivery in river basins. *Water Resour Res* **50**, 3826–3851 (2014).
64. Lee, D. & Veizer, J. Water and carbon cycles in the Mississippi River basin: Potential implications for the Northern Hemisphere residual terrestrial sink. *Global Biogeochem Cycles* **17**, (2003).
65. Baker, D. G. & Kuehnast, E. L. Precipitation normals for Minnesota: 1941-1970. *Climate of Minnesota, Technical Bulletin* **314**, 1–16 (1978).
66. Tena, A., Batalla, R. J., Vericat, D. & López-Tarazón, J. A. Suspended sediment dynamics in a large regulated river over a 10-year period (the lower Ebro, NE Iberian Peninsula). *Geomorphology* **125**, 73–84 (2011).
67. Hansford, M. R., Plink-Björklund, P. & Jones, E. R. Global quantitative analyses of river discharge variability and hydrograph shape with respect to climate types. *Earth Sci Rev* **200**, 102977 (2020).
68. Martin, R. L. & Jerolmack, D. J. Origin of hysteresis in bed form response to unsteady flows. *Water Resour Res* **49**, 1314–1333 (2013).
69. Wentworth, C. K. A Scale of Grade and Class Terms for Clastic Sediments. *https://doi.org/10.1086/622910* **30**, 377–392 (1922).
70. Hack, J. T., Seaton, F. A. & Nolan, T. B. *Studies of Longitudinal Stream Profiles in Virginia and Maryland*. *United States Department of the Interior* (1957).
71. Gupta, P. K., Chauhan, S. & Oza, M. P. Modelling surface run-off and trends analysis over India. *J. Earth Syst. Sci.* **125**, 1089–1102 (2016).

Supplementary Information S1: Table of localities

Locality number	Locality name	Member	Northing	Easting	BGS Map Title
1.1	Amphitheatre	Rhondda	5138.7	-00333.6	248 Pontypridd
2.1	Lower Bwlch Mountain Road	Llynfi	5138.7	-00331.94	248 Pontypridd
2.2	Upper Bwlch Mountain Road	Rhondda	5138.55	-00332.12	248 Pontypridd
2.3	Welcome to the Valleys Sign	Rhondda	5138.4	-00332.09	248 Pontypridd
3.1	Top of Disused Mineral Railway	Hughes	5183.52	-00347.71	247 Swansea
3.2	Disused Mineral Railway (Below Mountain Coal)	Hughes	5138.46	-00348.06	247 Swansea
3.3	Kilvey Hill West	Llynfi	5137.60	-00354.91	247 Swansea
3.4	Kilvey Hill East	Llynfi	5137.60	-00354.80	247 Swansea
4.1	Darren Serth Quarry (First Storey)	Swansea	5143.73	-00356.95	230 Ammanford
4.2	Darren Serth Quarry (Round Corner)	Swansea	5143.78	-00356.86	230 Ammanford
4.3	Darren Serth Quarry (Second Storey)	Swansea	5143.72	-00356.95	230 Ammanford
5.1	Llanwonno Road Quarry	Brithdir	5140.24	-00322.43	248 Pontypridd
5.2	Llanwonno Road	Brithdir	5140.24	-00322.43	248 Pontypridd
5.3	Quarry Above Porth	Brithdir	5137.56	-00323.96	248 Pontypridd
6.1	Above Abercynon	Hughes	5139.47	-00319.88	248 Pontypridd
6.2	Mynydd Cilfach-yr-encil	Brithdir	5142.75	-00319.79	231 Merthyr Tydfil
6.3	Bridge Street	Rhondda	5136.71	-00323.034	248 Pontypridd
7.1	Nolton Haven North Cliff	Rhondda	5149.43	-00506.65	226/227 Milford
7.2	Maidenhall Point	Rhondda	5150.58	-00506.99	226/227 Milford

Table 1: The localities used for primary data collection and their locations.

S2: Localities and access (.kmz)

A Google Earth .kmz file showing each locality, represented stratigraphy, and access information.

S3: Primary field data

An excel workbook with all collected primary field data and statistical tests.

- S3a: Data log outlining distribution of collected data between localities
- S3b: Cross-set height distributions
- S3c: Maximum cross-set height measurements
- S3d: Accretion and bedding
- S3e: Package thicknesses
- S3f: Woody debris measurements

- S3g: CV of cross-sets associated with woody debris
- S3h: Statistical test on cross-set heights between Members
- S3i: Statistical test on CV between Members
- S3j: Statistical test on CV between debris-associated and non-debris-associated cross-sets

S4: Extended methodology

Scaling relationships obtained in order to extract median cross-set height from measurements of maximum cross-set height were as follows:

Member	Mean/max	N
Combined (Pennant Formation)	0.626	271
Swansea	0.625	49
Hughes	0.596	33
Brithdir	0.636	58
Rhondda	0.618	104
Llynfi	0.656	27

Table 2: The derived scaling ratios between mean and maximum cross-set height for each Member of the Pennant Formation, including the number, N, of cross-set height distributions obtained from each Member.

Formative flow depth, H, was calculated using the relationship established by Bradley and Venditti:[1]

$$H = 6.7h_d$$

(Eq. 6)

where the value of 6.7 is an approximation of a scalar range with 50% probability between 4.4 and 10.1.

Primary grain-size data were used to calculate palaeoslope using the method of Trampush et al[2] where:

$$logS = a_0 + a_1 logD_{50} + a_2 logH$$

(Eq. 6)

in which S is channel slope, D_{50} is the median grain-size, and constants $a_0 = -2.08 \pm 0.036$, $a_1 = 0.254 \pm 0.016$, and $a_2 = -1.09 \pm 0.044$. To propagate the errors included in the constants, 10^6 values were generated of each (Monte Carlo uncertainty propagation).

Channel width is an important metric due to its necessity in establishing a total discharge, as opposed to discharge per unit width. This permits quantification of discharge during bankfull events, which must be known in order to estimate flood capacities. However, channel width is difficult to constrain from outcrop. The method established by Greenberg et al[3] describes the widths of individual river threads, and was used due to higher sampling potential than direct measurements of outcrop width. Furthermore, outcrop width is an indicator of the maximum width of the channel belt, rather than individual river channels, the latter of which has greater utility in palaeohydrologic reconstructions. In the Greenberg et al[3] method, lateral accretion package widths are used to estimate the total width of the channel:

$$W_{bf} = (2.34 \pm 0.13) W_{bar}$$

(Eq. 7)

where W_{bf} is bankfull width, and W_{bar} is the width of a bar package, defined as the distance between the locations that mark the 95% values of the asymptotes formed by the lateral accretion package. Exemplar asymptotic bar packages are shown in Figure 4d. Width estimates were made in tandem with estimates of planform morphology and fluvial style[4,5] (*Parker*, 1976; *Lyster et al.*, 2022b), as it is implicit in the Greenberg et al[3] method that rivers are single- threaded.

The total width of outcrops, measured in Google Earth, was used to indicate an upper limit on the width of the total channel belt.

Flow velocity was calculated using Manning's equation:

$$U = \frac{1}{n} H^{\frac{2}{3}} S^{\frac{1}{2}}$$

(Eq. 8)

where n is Manning's constant, set as 0.03.[6] Water discharges were then estimated using $Q = UH$ to obtain discharge per unit width (i.e., unit discharge, Q), and channel width, W_{bf}, was estimated (Eq. 7), to obtain bankfull discharge ($Q_{bf} = U\,H\,W_{bf}$).

Unit bedload flux, qb, was estimated using the methods of Mahon and McElroy[7]:

$$q_b = (1-\phi)\frac{h_d V_c}{2}$$

(Eq. 9)

$$logV_c = \beta_0 + \beta_1 logS$$

(Eq. 10)

where V_c is the bedform migration velocity, β_0 and β_1 are constants ($\beta_0 = 0.6113 \pm 0.144$, $\beta_1 = 1.305 \pm 0.0515$), and φ is a dimensionless bed porosity of 0.5.[7]

The flow intermittency factor, I_f, is defined as the fraction of the total time in which bankfull flow would accomplish the same amount of water discharge as the real hydrograph[8] (Equation 5). This metric is important for analysis of seasonality and intermittency of fluvial regimes. Flow intermittency requires estimating a yearly water budget, and this necessitates a range of assumptions. Based on atmospheric general circulation models[9,10] the palaeo-precipitation rate was estimated as between 1.5 and 2.5 mm/day (0.55 - 0.91 m/yr), and catchment area has been estimated as 500 - 1500 km^2 by Wood et al.[11] From these assumptions we have estimated the expected mean annual discharge, Q_a, for a given channel:

$$Q_a = Q_{wb}A$$

(Eq. 11)

where A is the catchment area, and Q_{wb} is the water budget, representing the water that enters the catchment as precipitation, assuming a 20% loss to infiltration and evaporation.[12]

S5: Sedimentary logs of crevasse splay deposit at Locality 4.3

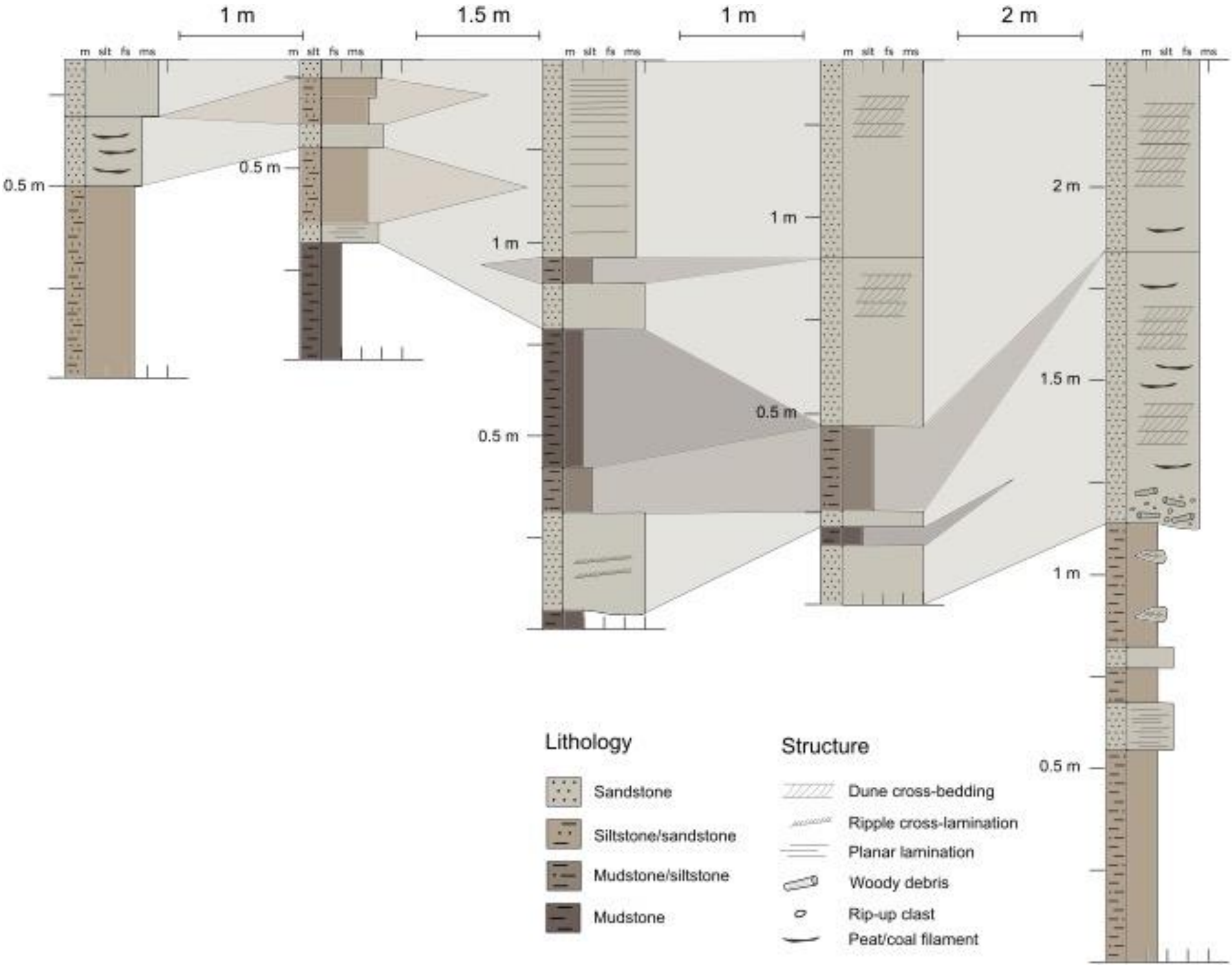

1. Bradley, R. W. & Venditti, J. G. Reevaluating dune scaling relations. *Earth-Science Reviews* **165**, 356–376 (2017).
2. T§rampush, S. M., Huzurbazar, S. & McElroy, B. Empirical assessment of theory for bankfull characteristics of alluvial channels. *Water Resources Research* **50**, 9211–9220 (2014).
3. Greenberg, E., Ganti, V. & Hajek, E. Quantifying bankfull flow width using preserved bar clinoforms from fluvial strata. *Geology* **49**, 1038–1043 (2021).
4. Parker, G. On the cause and characteristic scales of meandering and braiding in rivers. *J. Fluid Mech* **76**, 457–480 (1976).
5. Lyster, S. J., Whittaker, A. C. & Hajek, E. A. *The problem of paleo-planforms*. *Earth and Planetary Science Letters* (2022).
6. Lyster, S. J., Whittaker, A. C., Hajek, E. A. & Ganti, V. Field evidence for disequilibrium dynamics in preserved fluvial cross-strata: A record of discharge variability or morphodynamic hierarchy? *Earth and Planetary Science Letters* (2022).
7. Mahon, R. C. & McElroy, B. Indirect estimation of bedload flux from modern sand-bed rivers and ancient fluvial strata. *Geology* **46**, 579–582 (2018).

8. Hayden, A. T., Lamb, M. P. & McElroy, B. J. Constraining the Timespan of Fluvial Activity From the Intermittency of Sediment Transport on Earth and Mars. *Geophysical Research Letters* **48**, (2021).
9. Peyser, C. E. & Poulsen, C. J. Controls on Permo-Carboniferous precipitation over tropical Pangaea: A GCM sensitivity study. *Palaeogeography, Palaeoclimatology, Palaeoecology* **268**, 181–192 (2008).
10. Tabor, N. J. & Poulsen, C. J. Palaeoclimate across the Late Pennsylvanian-Early Permian tropical palaeolatitudes: A review of climate indicators, their distribution, and relation to palaeophysiographic climate factors. (2008) doi:10.1016/j.palaeo.2008.03.052.
11. Wood, J., McLeod, J. S., Lyster, S. J. & Whittaker, A. C. Rivers of the Variscan Foreland: fluvial morphodynamics in the Pennant Formation of South Wales, UK. *Journal of the Geological Society* (2022) doi:https://doi.org/10.31223/X5TK94.
12. Gupta, P. K., Chauhan, S. & Oza, M. P. Modelling surface run-off and trends analysis over India. *J. Earth Syst. Sci.* (2016) doi:10.1007/s12040-016-0720-z.